On a Calculation of the Symmetric Circulation and Its Implications for the Role of Eddies[1]

Richard S. Lindzen

Division of Applied Sciences

Harvard University

Cambridge, MA 02138

[1]A lecture at NCAR's summer colloquium on the general circulation, July 1978.

On a calculation of the symmetric circulation and it implications for the role of eddies

1. Introduction

This lecture is primarily based on a pair of publications (Schneider and Lindzen, 1977; Schneider, 1977) which have been available for some time. They describe calculations of steady, axially symmetric circulations -- calculations originally motivated by an assortment of questions in tropical meteorology: Could cumulus momentum exchange produce the reversal of the pole to equator temperature gradient at the tropopause? Are surface temperature gradients more important than upper level heating in generating low level moisture convergence? Does latent heating produce a realistic Hadley circulation? What determines the extent of the Hadley circulation and the extent of the resulting flattening of latitudinal temperature gradients? Although these were the questions which motivated us, some of the results which emerged offered some surprising suggestions for the general circulation. Most notably, some of the results displayed plausible Hadley and Ferrel cells, subtropical jets (too strong), reasonable distributions of surface easterlies and westerlies (perhaps a bit weak), and a tropopause jump near thirty degrees latitude -- all without the explicit inclusion of eddies. The impression ones gets from recent studies of the general circulation (Lorenz, 1967) is that symmetric circulations could not possibly account for the above features of the general circulation and hence there was a logical necessity for eddies to sustain the observed features. To be sure, the real atmosphere does have eddies, but the above results suggest that their presence may not be essential to many of the most basic features of the general circulation. It is this possibility which motivates the present review of Schneider and Lindzen (1977) and Schneider (1977). However, knowing the original motivation may help one understand some of the approximations used in these papers.

2. Equations and assumptions

The purpose of the above mentioned studies was to calculate the axially symmetric response of the atmosphere to the zonally averaged observed surface temperature and to the zonally averaged release of latent heat due to deep convective precipitation. Even these preconditions require some discussion. We start with the surface temperature since we assumed that the thermal adjustment time for the ocean is much longer than it is for the atmosphere. Thus, at any instant we assume the atmosphere is in equilibrium with the surface. Such an approach does not serve to explain why the surface temperature (which is not in radiative equilibrium with the sun) is what it is. Eddy heat transport could be an important process in determining surface temperature, and hence may be implicit in our results -- but so may ocean heat transports concerning which we are quite ignorant. An important role in determining surface temperature is also played by evaporation. The heat thus lost to the surface is released in the atmosphere through condensation and precipitation. Self-consistency requires that if observed surface temperatures are used, observed latent heat release must be included. Similarly, one might expect higher tropical surface temperatures in a dry atmosphere.

Our basic equations are as follows:

$$\frac{\partial \phi}{\partial \zeta} = \frac{RT}{H_o} \qquad (1)$$

$$\frac{1}{a\ cos\theta}\frac{\partial}{\partial \theta}(v\ cos\theta) + e^{\zeta/H_o}\frac{\partial}{\partial \zeta}(e^{-\zeta/H_o}\,\omega) = 0 \qquad (2)$$

$$\frac{1}{a\ cos\theta}\, v\, \frac{\partial(u\ cos\theta)}{\partial \theta} \quad \omega\frac{\partial u}{\partial \zeta} - 2\ \Omega\ v\ sin\theta = F_x \qquad (3)$$

$$\frac{v}{a}\ \frac{\partial}{\partial \theta} + \omega\frac{\partial v}{\partial \zeta} + 2\ \Omega\ u\ sin\theta + \frac{u^2\ tan\theta}{a} = -\frac{1}{a}\frac{\partial \phi}{\partial \theta} + F_y \qquad (4)$$

and

$$\frac{v}{a}\frac{\partial T}{\partial \theta} + \omega\left(\frac{\partial T}{\partial \zeta} + \Gamma\frac{T}{T_o}\right) = \frac{Q}{c_p} \qquad (5)$$

Equations (1) - (5) are simply the steady state equations for hydrostatic pressure, continuity, zonal momentum, meridional momentum and energy in log pressure coordinates. Notation is standard. For example, $\zeta = -H\ ln(P/P_o)$; $H_o = \frac{RT_o}{g}$; $\Gamma = \frac{g}{c_p}$; θ = latitude; a = earth's radius; and $\omega = \frac{d\zeta}{dt}$. Additional details may be found in Schneider and Lindzen (1977).

Details of modelling involve describing the momentum forcings F_x and F_y as well as the diabatic heating Q. Turbulent contributions to these quantities are given by

$$F_{xT} = \frac{1}{\rho}\frac{\partial}{\partial \zeta}\,\mu\,\frac{\partial u}{\partial \zeta} \qquad (6a)$$

$$F_{yT} = \frac{1}{\rho}\frac{\partial}{\partial \zeta}\,\mu\,\frac{\partial v}{\partial \zeta} \qquad (6b)$$

$$\frac{Q_T}{c_p} = \frac{1}{\rho}\frac{\partial}{\partial\zeta}\left[K\left(\frac{\partial T}{\partial\zeta} + \Gamma\frac{T}{T_o}\right)\right] \tag{6c}$$

We take $\mu = K$; the distribution of $\mu(z)$ is shown in Figure 1a: the justification for this distribution is based entirely on tropical conditions. The surface region of high μ corresponds to the tropical mixed layer; the transition region wherein μ decreases to a relatively small interior value corresponds to the region of marked cloud detrainment at the bottom of the trade cumulus layer. Such a justification for $\mu(z)$ is clearly irrelevant outside the tropics -- though we do not anticipate great problems arising from its use outside the tropics.

A more important part of the diabatic heating is due to radiation which we model in terms of Newtonian cooling:

$$\frac{Q_{rad}}{c_p} = \frac{T_e(\theta,\zeta) - T}{\tau(\zeta)} \tag{7}$$

where

$$T_e = 0.5\ \{[T_o(y) - \Gamma\zeta] + |T_o(y) - \Gamma\ \zeta\ |\} \tag{8}$$

$$y = a\ sin\theta$$

and

$$T_o = \Delta T(1 - .4(\frac{y}{a})^2) \tag{9}$$

$$\Delta T = 100°C$$

$\tau(\zeta)$, the radiative relaxation time, is shown in Fig. 1b; Eqs. (8) and (9) are based on the calculations of Manabe and Möller (1961); our stratospheric temperature has been scaled to 0° and the stratosphere is isothermal. $T_e(\zeta)$ at the equator and at $\theta = 45°$ is shown in Fig. 1c.

The final contribution to diabatic heating is due to latent heat release in cumulonimbi. For this we adopt the form suggested in Arakawa and Schubert (1974)

$$Q_{con} = \frac{M_c(\theta,\zeta)}{\rho}\left(\frac{\partial T}{\partial \zeta} + \Gamma \frac{T}{T_o}\right) \tag{10}$$

Arbitrarily and somewhat inconsistently we choose for M_c (the cumulus mass flux) a fixed vertical distribution as shown in Fig. 1d. The value of M_c is chosen so that (10) will correspond to the latent heat released in convective precipitation. For most of our calculations we use a climatological distribution of precipitation shown in Figure 2 (actually the symmetric part of this distribution is used in most of the calculations described in this lecture; asymmetric results are shown in Schneider and Lindzen, and Schneider). Some calculations have also been performed where M_c is related to calculated low level convergence -- although total precipitation remains equal to that shown in Figure 2.

In including cumulus heating, we also take care to include momentum exchange by cumulus. Following Schneider and Lindze (1976) we use the following parameterization

$$F_{x_{cum}} = \frac{1}{\rho}\frac{\partial}{\partial \zeta}\{M_c(\theta,\zeta)(u - u_c(\theta,\zeta))\} \tag{11}$$

where u_c = zonal velocity of cloud air, which we will take to be approximately equal to u at $\zeta = 0$. The contribution of cumulus friction to F_y turns out to be negligible.

Having specified F_x, F_y and Q, Eqs. (1)-(5) are further simplified by using Eq. (2) to define a stream function ψ where

$$v = \frac{e^{\zeta/H_o}}{\cos\theta} \frac{\partial\psi}{\partial\zeta} \tag{12a}$$

$$\omega = -\frac{e^{\zeta/H_o}}{a\cos\theta} \frac{\partial\psi}{\partial\theta} \tag{12b}$$

Also $y = a \sin\theta$ proves a more convenient meridional coordinate than θ itself.

Before proceeding to the final form of our equations, we non-dimensionalize our equations by means of the following scalings: ζ by H_o; y by a; T, T_o by ΔT; μ by ν; u, u_c by U; ψ by Ψ; Γ by $\Delta T/H_o$; τ by t; and M_c by $\rho\Psi/a$, where ΔT is the vertical temperature contrast at the equator; ν is μ at $\zeta = 0$; t is τ at $\zeta = 0$; U is $R\Delta T/2\Omega a$; Ψ is EUH_o where $E = \nu/(2\Omega H_o^2)$; also $R_o = U/2\Omega a$ and $\lambda = 1/(2\Omega Et)$ are important non-dimensional parameters.

In non-dimensional form, the resulting equations are

$$R_o \underline{\underline{\left[\frac{1}{(1-y^2)^{1/2}} \frac{\partial\psi}{\partial\zeta} \frac{\partial}{\partial y}\left[u(1-y^2)^{1/2}\right] - \frac{\partial\psi}{\partial y}\frac{\partial u}{\partial\zeta}\right]}}$$

$$\underline{- \frac{y}{(1-y^2)^{1/2}} \frac{\partial\psi}{\partial\zeta}} = \underline{\frac{\partial}{\partial\zeta}\left(\mu \frac{\partial u}{\partial\zeta}\right)} + \underline{R_o \frac{\partial}{\partial\zeta}[M_c(u - u_c)]} \;, \tag{13}$$

the zonal momentum equation,

$$E^2 R_o \frac{\partial}{\partial\zeta}\left[e^{2\zeta}\frac{\partial\psi}{\partial\zeta}\frac{\partial}{\partial y}\left(\frac{1}{(1-y^2)^{1/2}}\frac{\partial\psi}{\partial\zeta}\right) - e^{\zeta}\frac{\partial\psi}{\partial y}\frac{\partial}{\partial\zeta}\quad\frac{e^{\zeta}}{(1-y^2)^{1/2}}\frac{\partial\psi}{\partial\zeta}\right]$$

$$+ y\frac{\partial u}{\partial\zeta} + R_o\frac{y}{(1-y^2)^{1/2}}\frac{\partial}{\partial\zeta}u^2 = -(1-y^2)^{1/2}\frac{\partial T}{\partial y}$$

$$+ \frac{E^2}{(1-y^2)^{1/2}}\frac{\partial}{\partial\zeta}\left\{e^{\zeta}\frac{\partial}{\partial\zeta}\left[\mu\frac{\partial}{\partial\zeta}\left(e^{\zeta}\frac{\partial\psi}{\partial\zeta}\right)\right]\right\}, \qquad (14)$$

the generalized thermal wind equation, and

$$R_o\left[\frac{\partial\psi}{\partial\zeta}\frac{\partial T}{\partial y} - \frac{\partial\psi}{\partial y}\left(\frac{\partial T}{\partial\zeta} + \Gamma\frac{T}{T_o}\right)\right] = \frac{\partial}{\partial\zeta}\left[\mu\left(\frac{\partial T}{\partial\zeta} + \Gamma\right)\right]$$

$$+ \lambda e^{-\zeta}\frac{T_e - T}{\tau} + R_o M_c\left(\frac{\partial T}{\partial\zeta} + \Gamma\frac{T}{T_o}\right), \qquad (15)$$

the thermodynamic energy equation.

In the results described here, Eqs. (13)-(15) were not solved in their entirety. The terms underlined by ____ represent linear terms which are retained in all our calculations. The terms underlined by _ _ _ _ (in the zonal momentum equation) are nonlinear terms retained in some of our calculations. The terms underlined by ∿∿∿ represent nonlinear terms which are not included in calculations shown here but which appear to be of limited importance. The terms underlined by ^^^^^ are terms retained which involve the static stability. In these terms the static stability is fixed at essentially observed values as shown in Fig. 1e rather than calculated.

It may be argued that we should calculate static stability so as to maintain full internal consistency. Otherwise, the calculated temperature may imply a static stability other than that imposed. However, the choice of procedures is not so obvious. Clearly, in calculating the response of the atmosphere to thermal forcing, the static stability is an important determinant of the response. Thus, in using the observed stability one may be calculating the actual response even if that response is not maintaining the static stability. To state matters a bit differently, if one were to calculate the symmetric response self-consistently and find the static stability to be different from the observed stability, then one could conclude not only that the actual static stability were not maintained by the symmetric system, but also that the calculated symmetric circulation was not similar to the actual symmetric circulation. If, on the other hand, one used the observed stability in Eq. (15) and calculated a temperature inconsistent with the assumed stability, then one could again conclude that the symmetric circulation did not maintain the observed stability. However, in this case the calculated symmetric circulation should be close to that forced by diabatic heating in the real atmosphere. Thus there appears to be some advantage to the inconsistent approach. Such paradoxical situations arise commonly when one attempts to deal with individual components of nonlinear systems. In practice we will find that the assumed stability is consistent with the calculated stability in the domain of the Hadley circulation, but not outside this domain.

There now remains only the specification of boundary conditions. Because we are not dealing with wave propagation, no harm comes from assuming a top to our domain at $\zeta = \zeta_T = 2.6$. Our boundary conditions are then as follows:

$$\psi = 0 \text{ at } \zeta = 0, \zeta_T; \; y = \pm 1 \qquad (16)$$

$$\frac{\partial u}{\partial \zeta} = \frac{\partial}{\partial \zeta} e^{\zeta} \frac{\partial \psi}{\partial \zeta} = 0 \text{ at } \zeta = \zeta_T \qquad (17)$$

$$T = 0 \text{ at } \zeta = \zeta_T \qquad (18)$$

$$T = T_o(y) \text{ at } \zeta = 0 \qquad (19)$$

$$\left.\begin{aligned} \frac{\mu}{\rho(o)} \frac{\partial u}{\partial \zeta} &= c_D \, u \, |\underset{\sim}{v}| \\ \frac{\mu}{\rho} \frac{\partial v}{\partial \zeta} &= c_D \, v \, |\underset{\sim}{v}| \end{aligned}\right\} \text{ at } \zeta = 0, \qquad (20)$$

where $c_D = 10^{-3}$ and $|\underset{\sim}{v}|$ is set equal to $5 \; ms^{-1}$.

Note that (16) with (13) imply $u = 0$ at $y = \pm 1$. Also, for forcing symmetric about the equator, Eq. (13) implies $u = 0$ at $y = 0$. This last result depends on the presence of friction. Indeed, it may be shown more generally that (13) together with the above boundary conditions implies that zonal angular momentum can only have an extremum at the surface over the equator -- and that maximum must correspond to zero relative zonal velocity. A detailed discussion and derivation of this extended version of Hide's theorem is given in Schneider (1977). A rough derivation is given in Section 4 of the present paper.

3. Results

In this section I will select a subset of the results in Schneider and Lindzen and Schneider which illustrate the role of various processes and which display all the features we wish to stress -- even though the results differ somewhat from the most realistic calculations. Details of the calculations may be found in Schneider and Lindzen and Schneider. In the calculations presented, latent heating (when included) consists only in the symmetric component of the precipitation distribution shown in Fig. 2 -- or rather the symmetric part as approximated by the following formula:

$$P(y) = 190 \ cm \ yr^{-1} \ exp \ - \left(\frac{|y| - 0.1}{0.3}\right)^2 \ . \qquad (21)$$

In our first case we use the linearized versions of Eqs. (13)-(15). Moreover, we omit both latent heating (Eq. (10)) and its associated momentum transfer (Eq. (11)). The solution is forced by surface temperature (i.e., Eq. (9)). The resulting contours for zonal velocity, stream function and temperature are shown in Figs. 3, 4 and 5. The temperature is very nearly equal to T_e (viz Eqs. (8) and (9)), while the zonal wind is almost in thermal wind balance with the temperature. Only in a small neighborhood of the equator (about 10°) is the temperature variation with y flattened so as to produce $u = 0$ at $y = 0$. This is discussed further in Section 4. Significant meridional circulations are restricted to the neighborhood of the lower boundary where frictional effects are strong (viz Eq. (6)), though a weaker meridional circulation exists at all heights in the neighborhood of the equator. Note that the calculated stability for this case is much less than that observed (and employed in Eq. (15)).

In our next case we continue to use the linearized versions of Eqs. (13)-(15), but this time we include climatological latent heating (Eqs. (10) and (21)) but not the associated momentum transfer. Since this heating is deposited above the frictional boundary layer it gives rise to little additional meridional circulation beyond that found in the first case. The distributions of zonal velocity and temperature for this case are shown in Figs. 6 and 7. The temperature in Fig. 7 results primarily from a balance between latent heating (Eq. (10)) and radiative cooling (Eq. (7)) leading to a static stability in the tropics more nearly in line with our assumed stability. The zonal wind is essentially in thermal wind balance with this temperature. As in our first case a small meridional circulation exists in the neighborhood of the equator to produce zero zonal wind there. Whereas the zonal wind in the first case is of a magnitude similar to that observed (though the maximum is too close to the equator), the wind in this case is much larger (280 m/s).

In our third case we still use the linearized versions of Eqs. (13)-(15) but now we include both climatological latent heating and its associated momentum transfer (Eq. (11)). The resulting contours for zonal velocity, stream function and temperature are shown in Figs. 8, 9 and 10. The cumulus momentum transfer now forces a meridional circulation (wherein advection of the earth's angular momentum balances the cumulus "friction") which we see in Fig. 9. This upper level meridional circulation closely resembles in both extent and intensity the observed Hadley circulation. In our calculations, it remains distinct from the low level circulation associated with surface temperature gradients and boundary layer turbulence.[1] The Hadley circulation serves to profoundly diminish meridional temperature gradients in the tropics and subtropics as can be seen in Fig. 10. This is intimately related to the reduction of zonal velcoities effected by cumulus "friction" as may be seen in Fig. 8. Indeed, cumulus friction leads to a slight reduction of zonal velocity with height at the uppermost levels, and this is associated with a slight minimum in temperature at upper levels over the equator. The zonal jet maximum velocity is reduced to 135 m/s and this maximum is moved poleward to the edge of the Hadley cell. The Hadley cell extends to thirty degrees and basically follows the meridional distribution of cumulus friction. A more detailed discussion of the extent of the frictional Hadley cell is given in Section 4. It should also be noted that the jet in Fig. 8 has greater absolute angular momentum at thirty degrees than at the equator thus violating Hide's theorem. This, however, is not surprising since the linearized equations do not conserve angular momentum.

To remedy the above we perform a fourth set of calculations which are identical to the preceding calculations but where the non-linear terms in Eq. (13) are included thus preserving conservation of

---

[1]This suggests that the convergence of moisture and the resulting distribution of cumulus convection are largely determined by surface temperature gradients.

angular momentum.[2] Contours of zonal velocity, streamfunction and temperature for this case are shown in Figs. 11, 12 and 13. We see from Fig. 11 that winds equatorward of 30° are substantially reduced from their values in Fig. 8. The jet maximum is moved poleward and is actually stronger than in the linear calculations. Despite this, Hide's theorem is satisfied in this case. Moreover, meridional advection of relative momentum allows surface winds, and we now obtain a reasonable distribution of surface easterlies and westerlies with magnitude of about 4-5 m/s, which are probably a little less than observed values. It should be noted that the excessive strength of the upper level jet is diminished in more realistic pole to pole calculations (see Schneider, 1977), and would be further diminished by the inclusion of the centrifugal term in Eq. 13. But, in all calculations involving the present physics the jet strength remains too strong. In Fig. 12 we see that our meridional circulation now consists in a somewhat stronger and more extensive Hadley circulation as well as a Ferrel cell. The Hadley cell serves to supply the westerly momentum needed to balance surface friction in midlatitudes; the momentum is transferred to the Ferrel cell through turbulent diffusion, and the Ferrel cell then carries it to the surface. In the present configuration, it appears that the Ferrel cell arises from the frictional

---

[2]Doing over the first case with these nonlinearities included leads to almost no change. This is generally the case when the linear solution does not violate Hide's theorem.

response in the boundary layer to the surface pressure maximum at 30°.[3] From Fig. 13 we see that horizontal temperature gradients are again flattened over the extent of the Hadley cell. As in Fig. 10, the cumulus heating elevates the tropopause over the tropics with an apparent tropopause jump near 40°. The tropopause and temperature field norther of 40° are close to our assumed radiative equilibrium profile.

As concerns the last two cases, one may reasonably conclude that the inclusion of nonlinearity in Eq. (13) produces only small changes from the linear results with cumulus friction -- especially as concerns the extent and intensity of the Hadley cell. However, Schneider (1977) performed some calculations with a narrower (in latitude) concentration of precipitation but the same total latent heating. In these calculations there was virtually no cumulus friction outside the precipitation region. Nevertheless, the resulting Hadley circulations were still of the same magnitude and extent as in the above described calculations. Clearly, without friction nonlinear advection assumes a more major role.

4. On the extent of the Hadley circulation

As noted in Section 3, both cumulus friction and nonlinear momentum advection can independently lead to Hadley circulations of similar characteristics. The purpose of this section is to provide a crude analysis in support of this observation.

---

[3]To be sure, in the present *log p* coordinates the lower boundary is a constant *p* surface. However, the transition from easterlies to westerlies guarantees a pressure maximum on any constant height surface.

We will first consider the linear viscous model. Equation (13) becomes

$$\frac{\partial}{\partial \zeta}\left(\mu\frac{\partial u}{\partial \zeta}\right) + R_o \frac{\partial}{\partial \zeta}[M_c u] + \frac{y}{(1-y^2)^{1/2}} \frac{\partial \psi}{\partial \zeta} = 0 \tag{22}$$

where we have set $u_c = 0$.

Equation (22) may be integrated once to yield

$$\mu \frac{\partial u}{\partial \zeta} + R_o M_c u + \frac{y}{(1-y^2)^{1/2}} \psi = 0 \tag{23}$$

Equation (15) may be written

$$-R_o \sigma \frac{\partial \psi}{\partial y} = \alpha(\overline{T} - T) \tag{24}$$

where thermal diffusion has been ignored and where $\overline{T}$ is the temperature which results from equilibrium among the remaining diabatic terms. For simplicity we will take

$$\overline{T} = T_o(1 - b\, y^2) \tag{25}$$

It suffices for present purposes to use the following approximate thermal wind relation

$$\frac{\partial u}{\partial \zeta} = - \frac{(1 - y^2)^{1/2}}{y} \frac{\partial T}{\partial y} \tag{26}$$

For problems symmetric about the equator we must have

$$\psi \sim O(y) \tag{27}$$

Thus, Eq. (23) implies

$$u \sim O(y2), \tag{27}$$

and, using (28) we have from (26) that

$$T - T_{eq} \sim O(y4) \tag{29}$$

where T_{eq} is the temperature at $y = 0$. Equation (29) clearly shows that friction leads to a flattening of the temperature relative to what would be expected from Eq. (25) -- at least in the neighborhood of the equator. The extent of this neighborhood may be estimated as follows:

Assume the effects of friction are small. Then $\overline{u}$ will be a reasonable approximation to u, where

$$\frac{\partial \overline{u}}{\partial \zeta} \approx -\frac{1}{y}\frac{\partial \overline{T}}{\partial y} \tag{30}$$

and

$$\overline{u} \approx -\frac{1}{y}\frac{\partial \overline{T}}{\partial y} H \tag{31}$$

at some height H. If friction is considered as a simple perturbation then (23) implies

$$\psi \approx -\frac{1}{y}\left[\frac{\mu}{H} + R_o M_c\right] \overline{u}$$

$$\approx \frac{1}{y^2}\left[\frac{\mu}{H} + R_o M_c\right] \frac{\partial \overline{T}}{\partial y} H$$

$$\approx -\frac{1}{y^2}\left[\frac{\mu}{H} + R_o M_c\right] 1\ H\ T_o\ b\ y$$

$$\approx -\frac{2H\ T_o\ b}{y}\left[\frac{\mu}{H} + R_o M_c\right] \tag{32}$$

and

$$T \approx \overline{T} + \frac{R_o \sigma}{\alpha}\frac{\partial \psi}{\partial y}$$

$$\approx T_o - b\ T_o\ y^2 + \frac{R_o \sigma}{y^2}\left[\frac{\mu}{H} + R_o M_c\right] \frac{2H\ T_o\ b}{\alpha} \tag{33}$$

A rough scale for the extent of the region over which Hadley cell heat transports are important is obtained by finding that y where the last two terms in (33) are comparable:

$$y_b^4 \approx \frac{R_o \sigma [\frac{\mu}{H} + R_o M_c] 2H}{\alpha} \tag{34}$$

We see from (34) that the width of this region increases with the intensity of forcing (as measured by R_o), the basic static stability, the frictional coefficients and inversely with the diabatic thermal adjustment rate. Clearly, if the frictional processes, themselves, cease before $y = y_b$ then (33) is irrelevant. It should finally be noted that y_b is not necessarily the same as the extent of the Hadley circulation.

For the nonlinear case it proves convenient to rewrite Eq. (13) as follows:

$$R_o \left(\frac{\partial \hat{u}}{\partial y}\frac{\partial \psi}{\partial \zeta} - \frac{\partial \hat{u}}{\partial \zeta}\frac{\partial \psi}{\partial y}\right) = \frac{\partial}{\partial \zeta}\left(\mu \frac{\partial \hat{u}}{\partial \zeta}\right) + R_o \frac{\partial}{\partial \zeta}[M_c(\hat{u} - \hat{u}_c)], \tag{35}$$

where

$$\hat{u} = -\frac{1}{2} y^2 + R_o(1 - y^2)^{1/2} u . \tag{36}$$

$\hat{u}$ is a convenient measure of angular momentum. Equation (35) leads immediately to the previously cited Hide's theorem. We simply assume that $\hat{u}$ has a maximum somewhere. Then there will exist contours of constant $\hat{u}$. If we integrate (35) about such a contour, conservation of mass will lead to the contribution from the advection going to zero. We are then left with only the frictional terms. If these terms act to carry momentum down gradient then they will act to drain angular momentum from the maximum, and the existence of an interior maximum in $\hat{u}$ is inconsistent. Only at the ground over the equator is a maximum permitted.

For present purposes we note that if frictional terms are small, (35) implies conservation of $\hat{u}$ along stream lines. Assuming $u = 0$ at $y = 0$, we then have that along the upper branch of the Hadley cell,

$$u \simeq \frac{y^2}{2R_o} \tag{37}$$

and

$$\frac{\partial u}{\partial \zeta} \approx \frac{y^2}{2HR_o}$$

From the thermal wind relation we then get

$$\frac{\partial T}{\partial y} \approx \frac{y^3}{2HR_o}$$

and

$$T = T_{eq}(\zeta) - \frac{y^4}{8HR_o} . \tag{38}$$

Thus we see that in the absence of friction we have conservation of angular momentum; and in order for conservation of angular momentum to be consistent with thermal wind balance, temperature variation with latitude must be flatter than it is for $\overline{T}$. To determine the extent of a nonlinear Hadley cell we merely compare $\overline{u}$ as calculated from (30) and (25) with u from (37). For the former we have

$$\overline{u} \approx 2b\, T_o\, H,$$

and

$$y_{bnl}^2 \approx 4\, R_o\, b\, T_o\, H; \tag{39}$$

i.e., the Hadley cell acts to eliminate zonal velocities which are larger than what one would obtain from assuming conservation of angular momentum. Clearly when y_{bnl} (Eq. (38)) substantially exceeds y_b (Eq. (34)) the Hadley cell will be dominated by nonlinear transports. This corresponds to the case when precipitation and friction are confined to narrow regions. On the other hand, for the cases involving climatological distributions of precipitation y_{bnl} is only slightly larger than y_b, and the viscous results are a fair approximation of the more complete results. It should be mentioned, incidentally, that (39) is a very crude and sometimes inaccurate estimate. A more careful estimate is found in Schneider (1977). (See also lectures by I. Held and A. Hou in this volume.)

4. Concluding remarks

In many, if not all, recent studies of the general circulation of the atmosphere (see Lorenz, 1967; Oort and Rasmussen, 1971), one is led to believe that such features as the surface westerlies of middle latitudes and the jet stream are due to eddy fluxes. If this represents a realistic assessment of the role of eddies, then on would expect that in the absence of eddies, the general circulation would consist in at least a diminished jet stream and reduced surface westerlies. The present calculations do not support this view to any significant extent. In the absence of eddies, our calculations suggest that the symmetric circulations forced by radiative exchange with the surface and by latent heat release will maintain slightly smaller than observed easterlies and westerlies, Hadley and Ferrel cells differeing somewhat from observations in shape and intensity, and a jet stream which is too strong. It is, moreover, readily shown (see Schneider, 1977) that cumulus convection maintains the observed static stability in the tropics, though the present models fail to predict correct static stabilities in higher latitudes. This last failure and the overestimation of jet speeds are the two main shortcomings in our symmetric calculations.

In connection with the above, it is interesting to note some recent unpublished calculations by E. Schneider. In these he inserted as additional forcing terms for the symmetric calculations the $\overline{u'v'}$ and $\overline{v'T'}$ fluxes from Oort and Rasmussen (1971). These fluxes forced modifications of both the Hadley and Ferrel cells which yielded circulations closer to those observed. However, they produced almost no change in the jet magnitude; nor did they correct midlatitude static stabilities. Surface winds were increased to values in excess of those observed. On the other hand, when Schneider introduced $\overline{\omega'T'}$ fluxes from observational analyses by Newell, *et al.* (1972), these fluxes resulted in substantially more correct static stabilities and jet strength, the latter correction being intimately related to the former (i.e., correcting midlatitude static stability greatly reduced horizontal temperature gradients at the boundary of the Hadley cell). The tentative conclusion we reach from all the above is that the basic role of atmospheric eddies is the maintenance of static stabilities at middle and high latitudes and possibly the maintenance of surface temperature gradients between the tropics and the poles. They may play a significant role in the maintenance of surface winds, and they probably inhibit the jet stream.

Acknowledgement

The author was supported by NSF Grant No. ATM-20156 during the preparation of this lecture. Correspondence with E. Schneider is gratefully acknowledged as are conversations with I. Held and A. Hou.

References

Arakawa, A. and W. H. Shubert, 1974: Interaction of a cumulus cloud ensemble with the large scale environment, Part I. J. Atmos. Sci., 31, 674-701.

Lorenz, E. N., 1967: The Nature and Theory of the General Circulation in the Atmosphere. W.M.O. Publ. No. 218, T.P. 115, 161 pp.

Manabe, S. and F. Möller, 1961: On the radiative equilibrium and heat balance of the atmosphere. Mon. Wea. Rev., 89, 503-532.

Newell, R. E., J. E. Kidson, D. G. Vincent, and G. J. Boer, 1972: The General Circulation of the Tropical Atmosphere, Vol. II. The MIT Press, 371 pp.

Oort, A. H. and E. M. Rasmusson, 1971. Atmospheric Circulation Statistics. NOAA Prof. Paper No. 5, U.S. Gov't. Printing Office, Washington, D.C., 323 pp.

Schneider, E. K., 1977: Axially symmetric steady-state models of the basic state for instability and climate studies. II, Nonlinear calculations. J. Atmos. Sci., 34, 280-296.

Schneider, E. K. and R. S. Lindzen, 1977: Axially symmetric steady-state models of the basic state of instability and climate studiess. I, Linear calculations. J. Atmos. Sci., 34, 263-279.

Figure Legends

Figure 1. a) Eddy viscosity v. height.

b) Radiative relaxation time v. pressure.

c) Radiative equilibrium temperature v. height for equator and 45° latitude.

d) Cumulus mass flux (normalized) v. pressure.

e) Assumed static stability v. height.

Figure 2. Zonal mean cumulus precipitation.

Figure 3. Contours of zonal wind for first case (contour interval $10\ ms^{-1}$).

Figure 4. Streamfunction contours for first case (contour interval $10^{13} gs^{-1}$).

Figure 5. Temperature contours for first case (contour interval $10\ K$).

Figure 6. Contours of zonal wind for second case (contour intervals $40\ ms^{-1}$).

Figure 7. Temperature contours for second case (contour intervals $10\ K$).

Figure 8. Zonal wind contours for third case (contour intervals $15\ ms^{-1}$).

Figure 9. Streamfunction contours for third case (contour intervals $10^{13} gs^{-1}$).

Figure 10. Temperature contours for third case (contour intervals $10\ K$).

Figure 11. Zonal wind contours for fourth case (contour intervals $15\ ms^{-1}$).

Figure 12. Streamfunction contours for fourth case (contour intervals $10^{13} gs^{-1}$).

Figure 13. Temperature contours for fourth case (contour intervals $10\ K$).

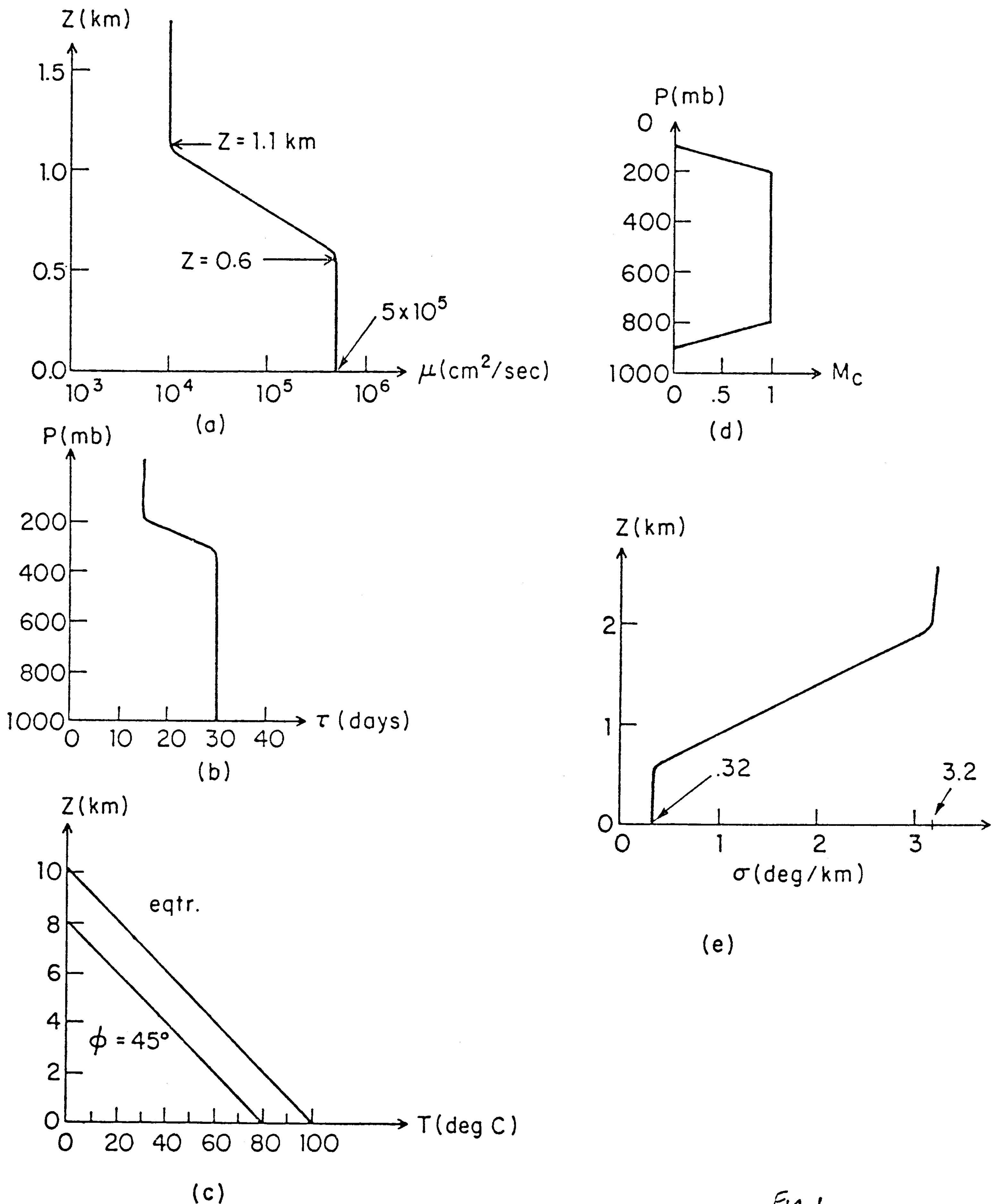

Z(km)
1.5
1.0
0.5
0.0
Z = 1.1 km
Z = 0.6
5x10^5
10^3 10^4 10^5 10^6
μ(cm^2/sec)
(a)
P(mb)
200
400
600
800
1000
0 10 20 30 40
τ (days)
(b)
Z(km)
10
8
6
4
2
0
eqtr.
φ = 45°
0 20 40 60 80 100
T(deg C)
(c)
P(mb)
0
200
400
600
800
1000
0 .5 1
M_c
(d)
Z(km)
2
1
0
.32
3.2
0 1 2 3
σ(deg/km)
(e)

FIG. 1

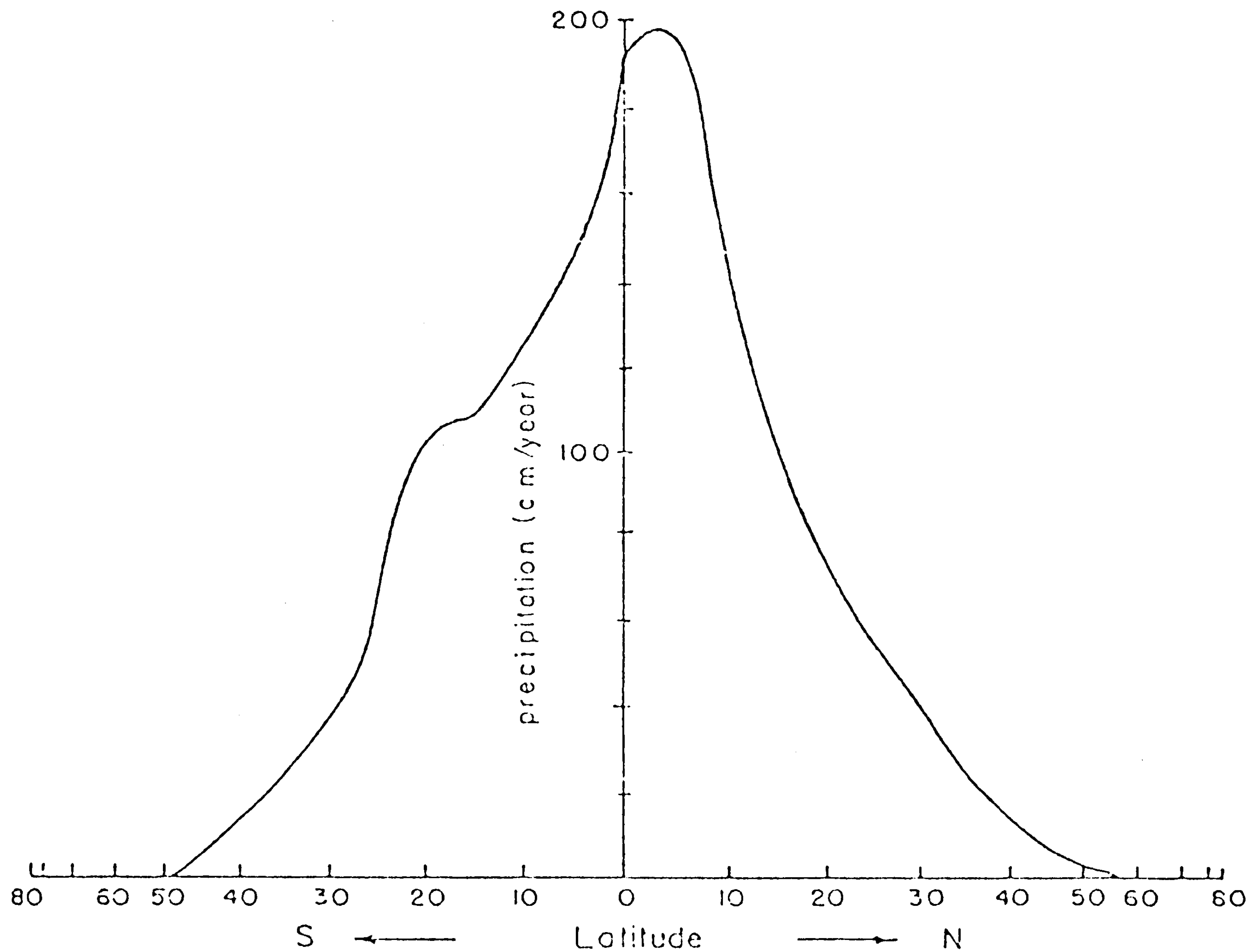
200
100
precipitation (cm/year)
80
60
50
40
30
20
10
0
10
20
30
40
50
60
80
S
Latitude
N

FIG. 2

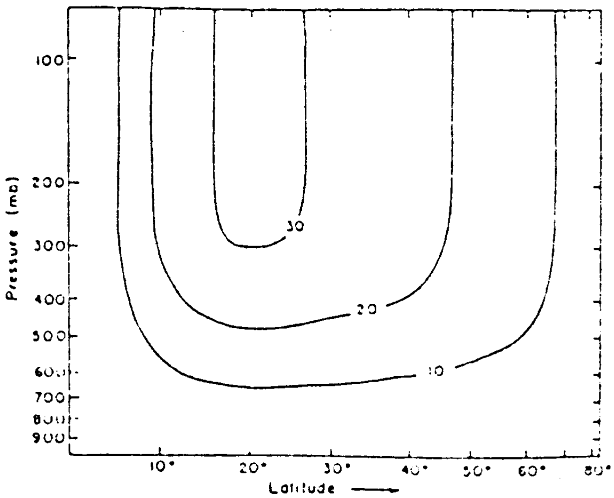

FIG. 3

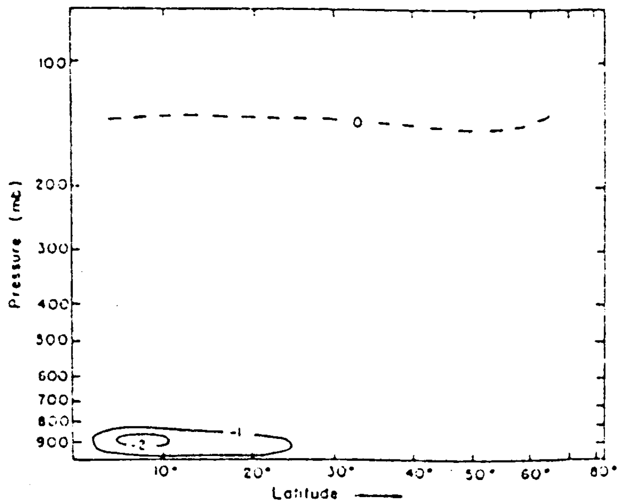

FIG. 4.

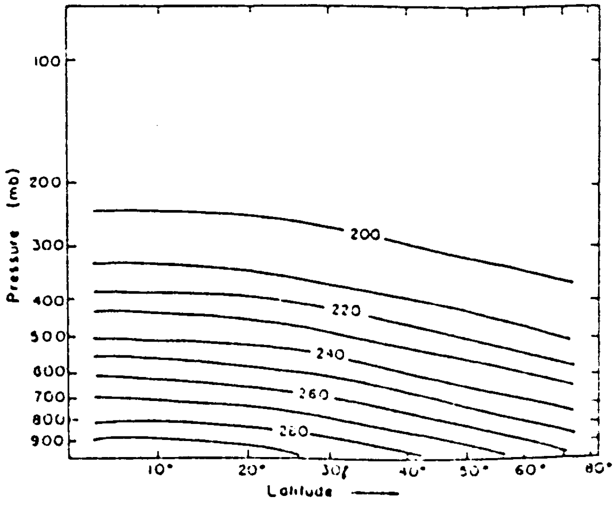

FIG. 5

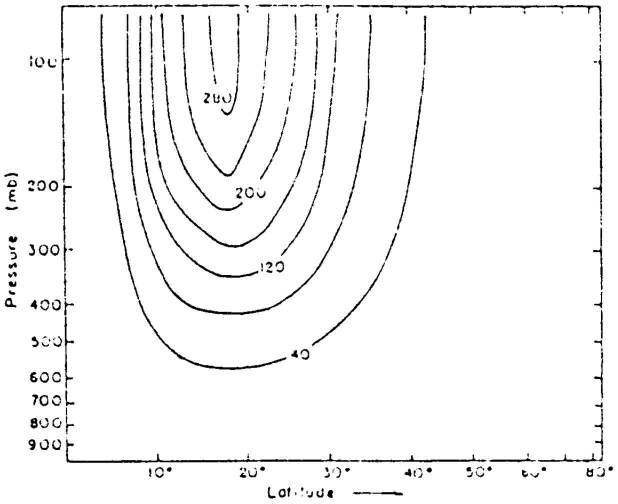

100
200
300
400
500
600
700
800
900
Pressure (mb)
280
200
120
40
10°
20°
30°
40°
50°
60°
80°
Latitude

FIG. 6

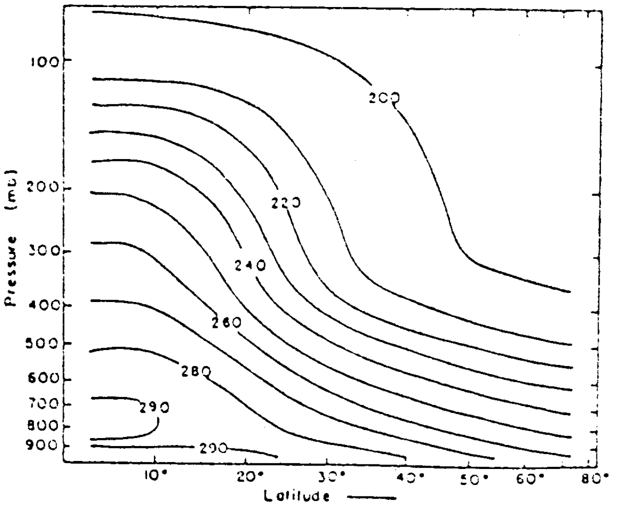

100
200
300
400
500
600
700
800
900
Pressure (mb)
200
220
240
260
280
290
290
10°
20°
30°
40°
50°
60°
80°
Latitude

FIG. 7

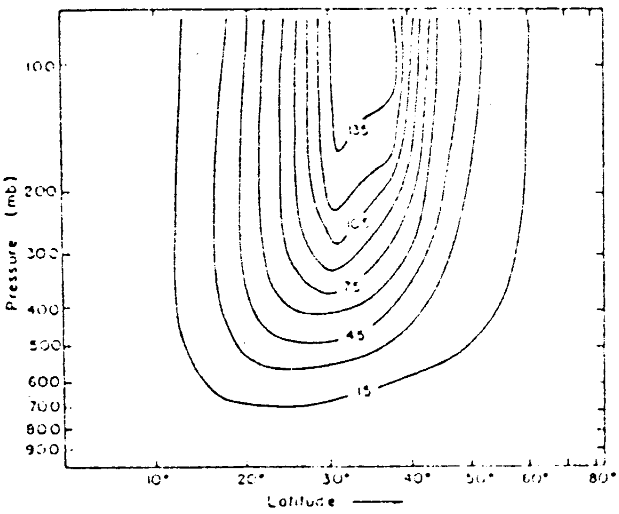

FIG. 8

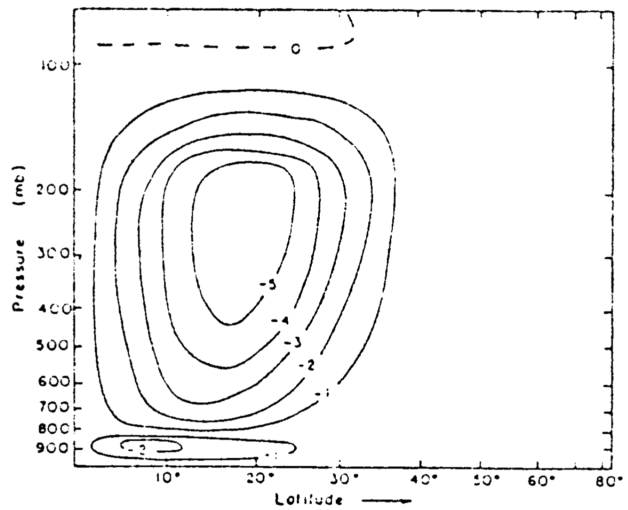

FIG. 9

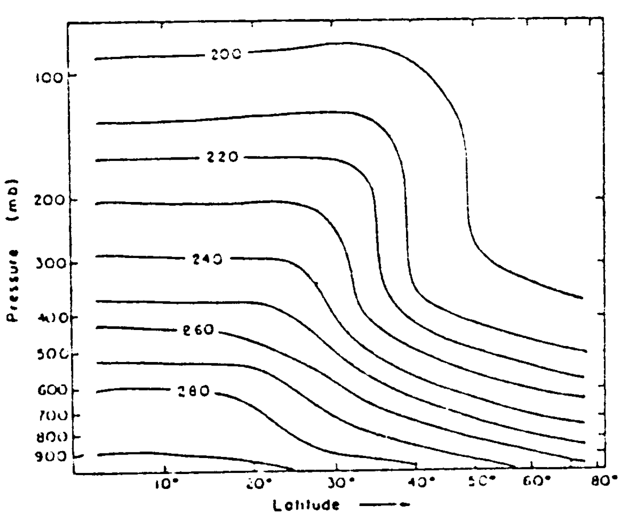

FIG 10

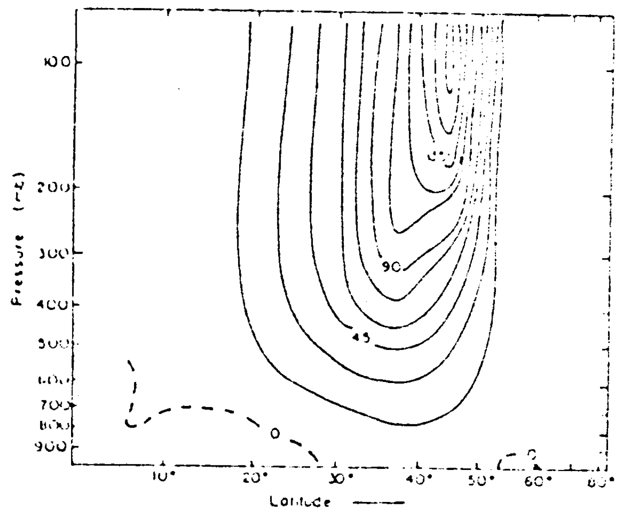

FIG. 11

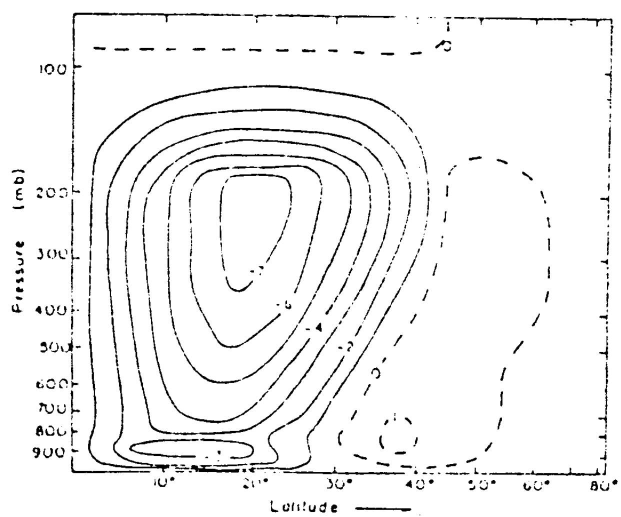

FIG. 12

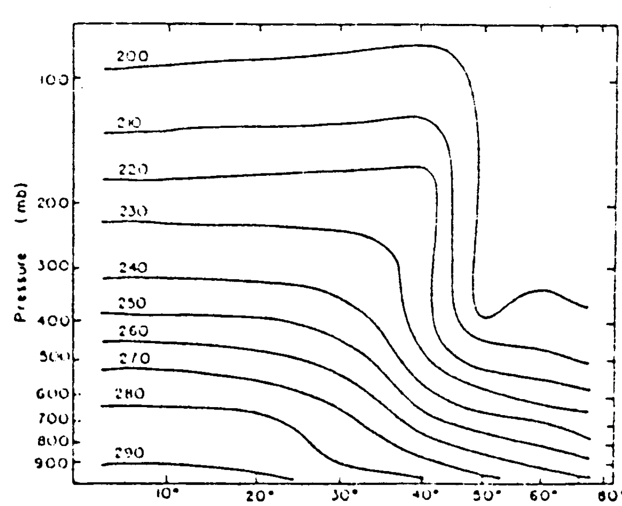

FIG. 13